



NRL/FR/7210--07-10,150

The NRL Long-Wavelength Test Array

K.P. STEWART

B.C. HICKS

P.C. CRANE

P.S. RAY

C. GROSS

E. POLISENSKY

A. COHEN

N.E. KASSIM

K.W. WEILER

*Radio, IR, and Optical Sensors Branch
Remote Sensing Division*

June 22, 2007

Approved for public release; distribution is unlimited.

REPORT DOCUMENTATION PAGE

Form Approved
OMB No. 0704-0188

Public reporting burden for this collection of information is estimated to average 1 hour per response, including the time for reviewing instructions, searching existing data sources, gathering and maintaining the data needed, and completing and reviewing this collection of information. Send comments regarding this burden estimate or any other aspect of this collection of information, including suggestions for reducing this burden to Department of Defense, Washington Headquarters Services, Directorate for Information Operations and Reports (0704-0188), 1215 Jefferson Davis Highway, Suite 1204, Arlington, VA 22202-4302. Respondents should be aware that notwithstanding any other provision of law, no person shall be subject to any penalty for failing to comply with a collection of information if it does not display a currently valid OMB control number. **PLEASE DO NOT RETURN YOUR FORM TO THE ABOVE ADDRESS.**

1. REPORT DATE (DD-MM-YYYY) 22-06-2007			2. REPORT TYPE Formal Report		3. DATES COVERED (From - To)	
4. TITLE AND SUBTITLE The NRL Long-Wavelength Test Array					5a. CONTRACT NUMBER	
					5b. GRANT NUMBER	
					5c. PROGRAM ELEMENT NUMBER	
6. AUTHOR(S) K.P. Stewart, B.C. Hicks, P.C. Crane, P.S. Ray, C. Gross, E. Polisensky, A. Cohen, N.E. Kasim, and K.W. Weiler					5d. PROJECT NUMBER	
					5e. TASK NUMBER	
					5f. WORK UNIT NUMBER	
7. PERFORMING ORGANIZATION NAME(S) AND ADDRESS(ES) Naval Research Laboratory 4555 Overlook Avenue, SW Washington, DC 20375-5320					8. PERFORMING ORGANIZATION REPORT NUMBER NRL/FR/7210--07-10,150	
9. SPONSORING / MONITORING AGENCY NAME(S) AND ADDRESS(ES) Office of Naval Research Suite 1425 875 North Randolph Street Arlington, VA 22203-1995					10. SPONSOR / MONITOR'S ACRONYM(S) ONR	
					11. SPONSOR / MONITOR'S REPORT NUMBER(S)	
12. DISTRIBUTION / AVAILABILITY STATEMENT Approved for public release; distribution is unlimited.						
13. SUPPLEMENTARY NOTES						
14. ABSTRACT The NRL Long-Wavelength Test Array (NLTA) was constructed to develop and test active baluns and electrically short dipoles for possible use as the primary wideband receiving elements for an emerging suite of large HF/VHF arrays including the Low Frequency Array (LOFAR) and the Long-Wavelength Array (LWA). Several dipoles of various designs and dimensions have been built and tested. Their useful range is when the dipoles arms are between approximately 1/8 and one wavelength long and the feedpoint is less than one half wavelength above ground. The NLTA, operating as an interferometer, has observed fringes from the brightest celestial sources in the frequency range from 10 to 50 MHz. The antenna temperatures vary from about 10% to 100% of the average brightness temperature of the Galactic background. With these parameters, it is relatively easy to make the amplifier noise levels low enough so that final system temperature is dominated by the Galactic background.						
15. SUBJECT TERMS Long-Wavelength Array (LWA)						
16. SECURITY CLASSIFICATION OF:				17. LIMITATION OF ABSTRACT UL	18. NUMBER OF PAGES 24	19a. NAME OF RESPONSIBLE PERSON Kenneth P. Stewart
a. REPORT Unclassified	b. ABSTRACT Unclassified	c. THIS PAGE Unclassified	19b. TELEPHONE NUMBER (include area code) (202) 767-2527			

CONTENTS

INTRODUCTION	1
HARDWARE	2
Antennas	2
Baluns	5
Data Collection Hardware.....	6
SOFTWARE.....	10
RESULTS	11
CONCLUSIONS.....	13
ACKNOWLEDGMENTS	14
REFERENCES	14
APPENDIX — NLTA Data Collection C Code.....	17

THE NRL LONG-WAVELENGTH TEST ARRAY

INTRODUCTION

The Naval Research Laboratory (NRL) Long-Wavelength Test Array (NLTA) was constructed to develop and test active baluns and electrically short dipoles for possible use as the primary wideband receiving elements for an emerging suite of large HF/VHF arrays including the Low Frequency Array (LOFAR) and the Long-Wavelength Array (LWA). Several dipoles of various designs and dimensions have been built and tested. Their useful range is when the dipole arms are between approximately one-eighth to one wavelength long and the feedpoint is less than half of one wavelength above ground. The NLTA, operating as an interferometer, has observed fringes from the brightest celestial sources in the frequency range from 10 MHz to 50 MHz. The antenna temperatures vary from about 10% to 100% of the average brightness temperature of the Galactic background. With these parameters, it is relatively easy to make the amplifier noise levels low enough so that final system temperature is dominated by the Galactic background.

The NLTA is comprised of eight antennas arranged in two four-element arrays separated by a distance of 218 m along an azimuth of 223.5° located at National Aeronautics and Space Administration/Goddard Space Flight Center (NASA/GSFC) in Greenbelt, MD. Signals from the four antennas within each array are summed, and the resulting signals from the arrays are combined to form a two-element interferometer. Interferometric fringes have been observed as the celestial sources transit through the beam response pattern of the arrays. This permits testing of theoretical models of antenna performance and development of signal processing hardware and software that will be needed for the LWA.

The LWA, together with the LOFAR, will be the first of a new generation of large, HF/VHF, multi-element, synthesis-imaging telescopes for radio astronomy at dekameter/meter wavelengths. The LWA will investigate the relatively unexplored frequency range between 20 and 80 MHz with unprecedented angular resolution and sensitivity, making it uniquely suited to serendipitous discovery, and also able to address a variety of scientific problems ranging in scale from the Earth's ionosphere to the most distant objects in the Universe. Three key science areas have been identified for the LWA: cosmic evolution, the acceleration of relativistic particles, and plasma physics. It will also be a powerful instrument for solar radio studies as well as ionospheric and space weather research [1,2]. Digital hardware and software will enable millisecond-timescale pointing and frequency agility, with multi-beaming capability allowing simultaneous, full-sensitivity observations in widely separated directions. The final system will involve thousands of dual-polarized dipole antennas and must therefore be inexpensive, simple, robust, and easy to manufacture and install. The NLTA serves as a test bed for developing hardware and software technology for the LWA.

HARDWARE

Antennas

Several different antenna designs were considered for the NLTA. Log periodic designs are attractive because their performance is approximately independent of frequency over a large bandwidth. But their beam width is generally too narrow to give adequate sky coverage for the LWA, and they are relatively difficult and expensive to build. Dipoles are easier to build and have broad beamwidth, but the large variation of feedpoint impedance with frequency requires a more complex active balun or matching network. Dipoles with “fat” arms of large cross section have less extreme and slower impedance variations with frequency than those with thin wire arms, but use of full 3-dimensional (3-D) fat dipoles as have been used in the UTR-2 [3] is too complex and expensive. We have constructed dipoles with 2-dimensional (2-D) arms of several sizes and shapes and found that, apart from wavelength scaling with size, response pattern differences were minor. Figure 1 is a drawing of the inverted-V dipole antennas used in the NLTA with the dimensions shown. Each dipole arm is constructed of four Cu tubes, forming a fat, planar dipole. The size was determined by the ready availability of 1.83 m (6 ft) long, 16 mm (5/8 in) O.D. Cu tubing. The design was chosen to minimize the labor involved in their construction without significantly degrading performance.

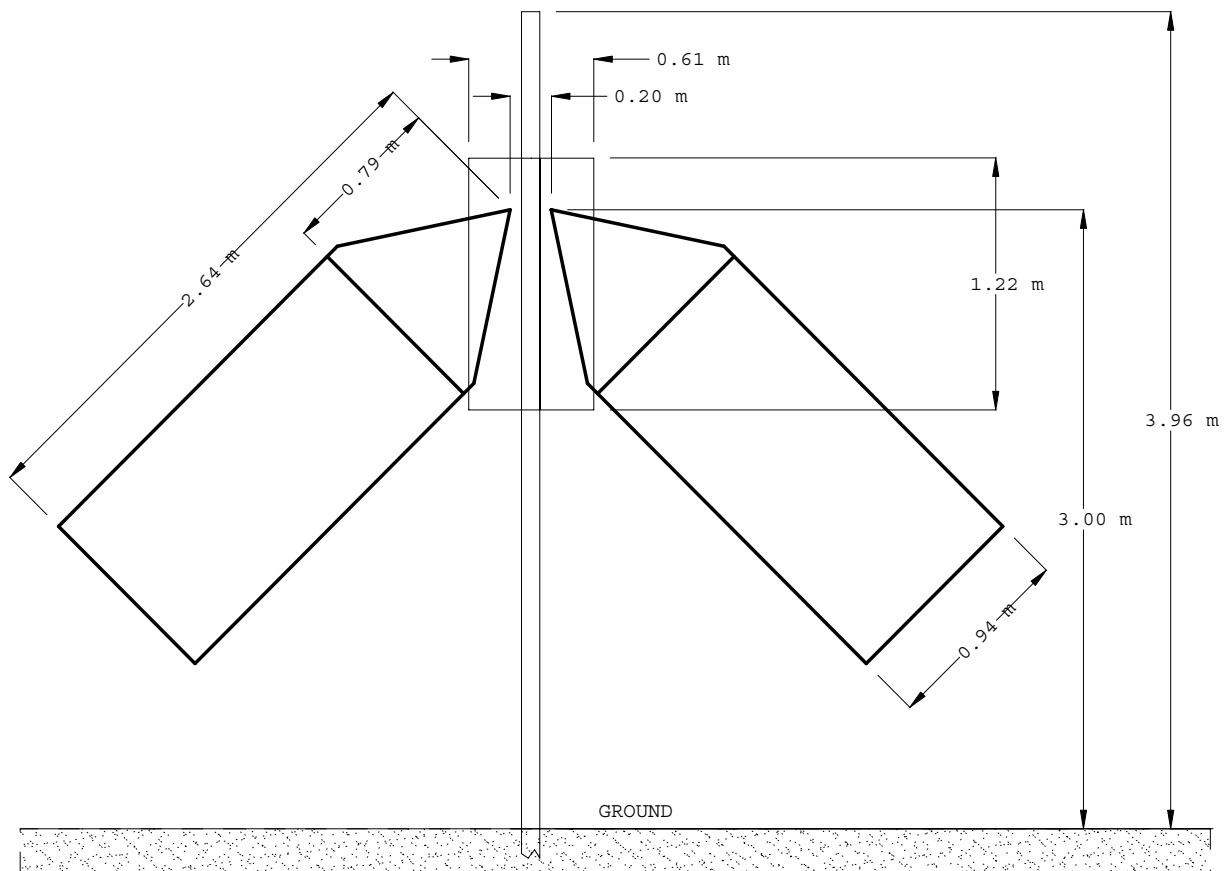


Fig. 1 — Drawing of the inverted-V dipole antennas. They are constructed of 16 mm diameter Cu tubing. The angle of the arms is 45° below horizontal.

The arms of the dipoles are inclined 45° below horizontal in order to increase the E-plane response at low elevations in an attempt to meet the LWA specification of 120° half-power beam width. The feedpoints are 3.0 m above the ground. The eight antennas are arranged in two four-element linear arrays, one running in the north-south direction, the other in the east-west direction (Figs. 2 and 3). The E-W array is 218 m southwest of the N-S array at azimuth 223.5° . The antenna site did not permit an exact E-W baseline between the arrays, which would have simplified the data reduction. The individual antennas in each array are 5.0 m apart. Although dual-polarized antennas are required by the LWA specifications, the NLTA dipoles are all single polarization aligned in the N-S direction, and presently are sensitive to only one polarization. Newer dual-polarized designs derived from the NLTA experience are being tested elsewhere.

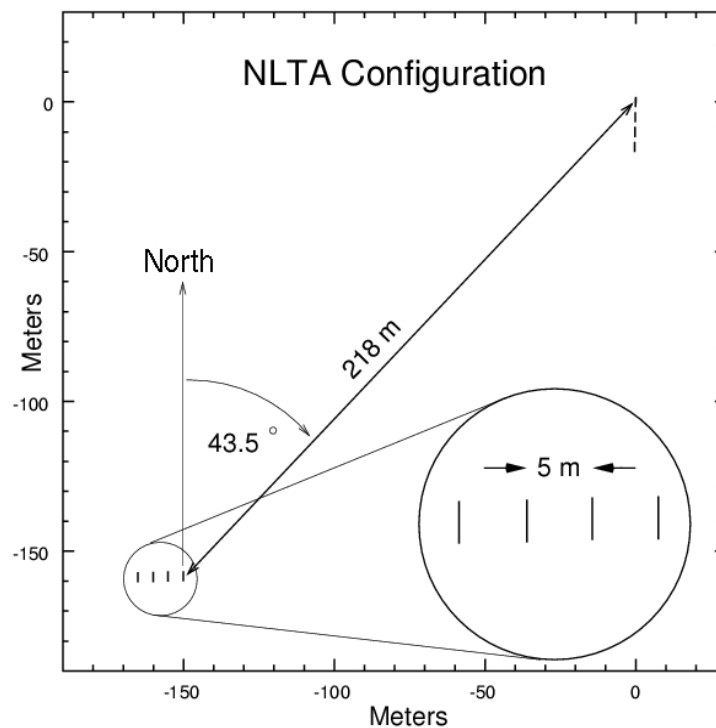


Fig. 2 — Relative positions of the NLTA antennas. In both arrays, the antenna feedpoints are 5.0 m apart. The control room is approximately 70 m north of the N-S array.

The antennas were mounted on 4×4 pressure-treated wooden posts 16 ft long. The dipole arms were positioned by fixing them to $24 \times 48 \times 3/4$ inch plywood sheets with plastic cable ties. The balun/preamp boxes were bolted to the plywood between the dipole arms and the plywood was bolted to the posts. Plywood was used to facilitate rapid construction of these prototype antennas. It would not be used for LWA production antennas. There was some concern that the plywood would affect the antenna properties, especially when it got wet; however, electromagnetic simulations predict that the antenna gain changes by less than 2 dB in the worst case, comparing free space, kiln-dried plywood, and fiber saturated plywood.



(a)



(b)

Fig. 3 — (a) N-S array, (b) E-W array

The response patterns of an individual antenna were calculated with the NEC2 antenna simulation code (www.nec2.org) and are shown in Fig. 4 for 25 MHz and 74 MHz. The conductivity and dielectric constant of the soil at the NLTA site were estimated to be 5 mS/m and 13, respectively. At 25 MHz the response is nearly isotropic in azimuth and has a beam width varying between 82° and 122° , which is close to the LWA specification. At 74 MHz, however, where the feedpoint is about $\frac{3}{4}$ wavelength above the ground, the response decreases at the zenith and the pattern develops undesirable low-angle side lobes.

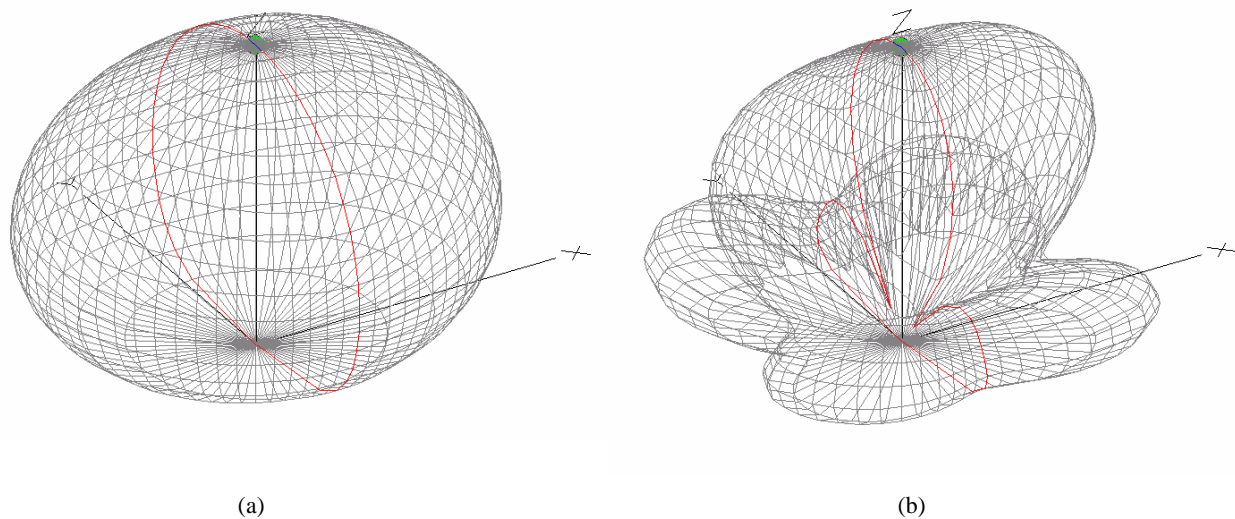


Fig. 4 — The calculated response patterns of the antennas at (a) 25 MHz and (b) 74 MHz over average ground. The dipole arms are in the y - z plane.

Baluns

The dipoles were tested with an active balun, i.e., a balun in which amplifiers are connected directly to the dipole arms in order to buffer the dipole impedance variations with frequency (Fig. 5). The active balun contains separate amplifiers for each arm of the dipole followed by a wideband balanced-to-unbalanced transmission line transformer. The use of separate amplifiers in a push-pull configuration greatly reduces even-order distortion products. The Motorola CA2830C wideband linear amplifier was chosen because of its low noise figure (5 dB), high dynamic range (output third order intercept = 46 dBm), and low distortion. Although this balun design provided a very useful proof-of-concept, its high cost and high power consumption (~ 10 W) make it unsuitable for use in the LWA, where thousands of units will be needed.

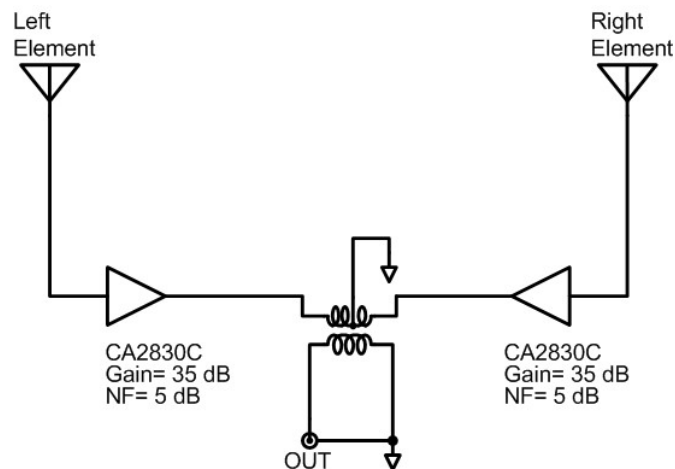


Fig. 5 — Schematic diagram of the active balun. The transformer gives an impedance step-down of 2:1.

One of the active baluns now installed in the NLTA antennas is shown in Fig. 6. The two Motorola amplifiers can be seen at the top of the weatherproof box. The actual balanced-to-unbalanced transformer is the gray Mini-Circuits (T-622) package visible in the center of the circuit board. A large heat sink (not visible in the picture) is mounted on the back of the box to dissipate the heat from the amplifiers.

The NLTA antenna/balun design has ultimately been very successful and has been reproduced for use in such ongoing programs as GASE [4], GDRT, GB/SRBS [5]. The performance of these and similar designs has been evaluated by Ellingson [6].

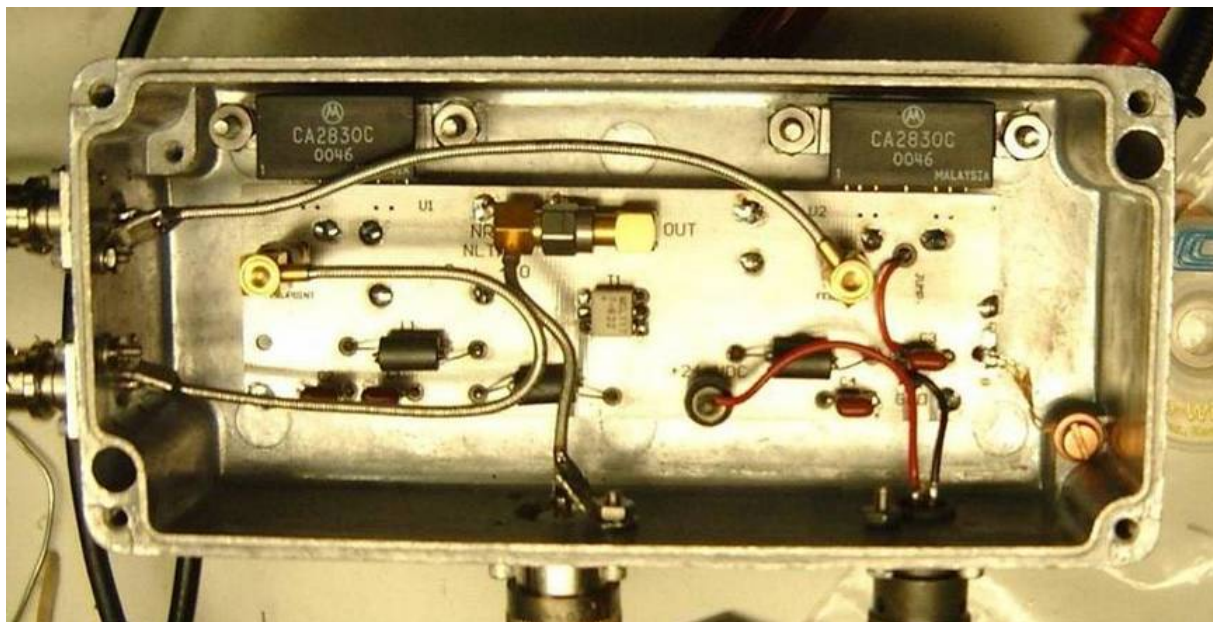


Fig. 6 — One of the active baluns used in the NLTA

Data Collection Hardware

The signals from the individual antennas in each of the four-element arrays are added together using three Mini-Circuits ZSC-2-1W power combiners. The combined response pattern of the four antennas is a fan beam perpendicular to the plane of the array. This gives the two signals required for interferometry: one from the N-S array and one from the E-W array. The product of the two perpendicular fan beams is a pencil beam pointed at the zenith. Additional time-delay phasing cables of length $n\Delta l$, ($n = 0, \dots, 3$) are inserted in the signal path before the power combiners to direct the beam away from the zenith as indicated in Fig. 7. The length Δl is given for any desired zenith angle θ by:

$$\Delta l = v_f d \sin \theta,$$

where d = distance between antennas and
 v_f = velocity factor of coaxial cable.

A 100-m long coaxial cable runs from each antenna in the N-S array into the control room. The power combiners are located in the control room to permit convenient shifting of the beam direction along the meridian, north or south of the zenith. For some observations RF switches are used to automate the beam pointing [7]. Because of the location of the E-W array, the power combiners are located at the antennas so

that only one coaxial cable is needed for the 420-m run back to the control room. Extra cable is inserted into the signal path of the closer N-S array to make the total path length equal for both arrays. This keeps the phase and signal losses the same for both arrays. Low-loss Times Microwave LMR-400 direct-bury cable (< 3 dB/100 m at 50 MHz) is used except for the time-delay phasing cables, where lighter, more flexible LMR-240 is used.

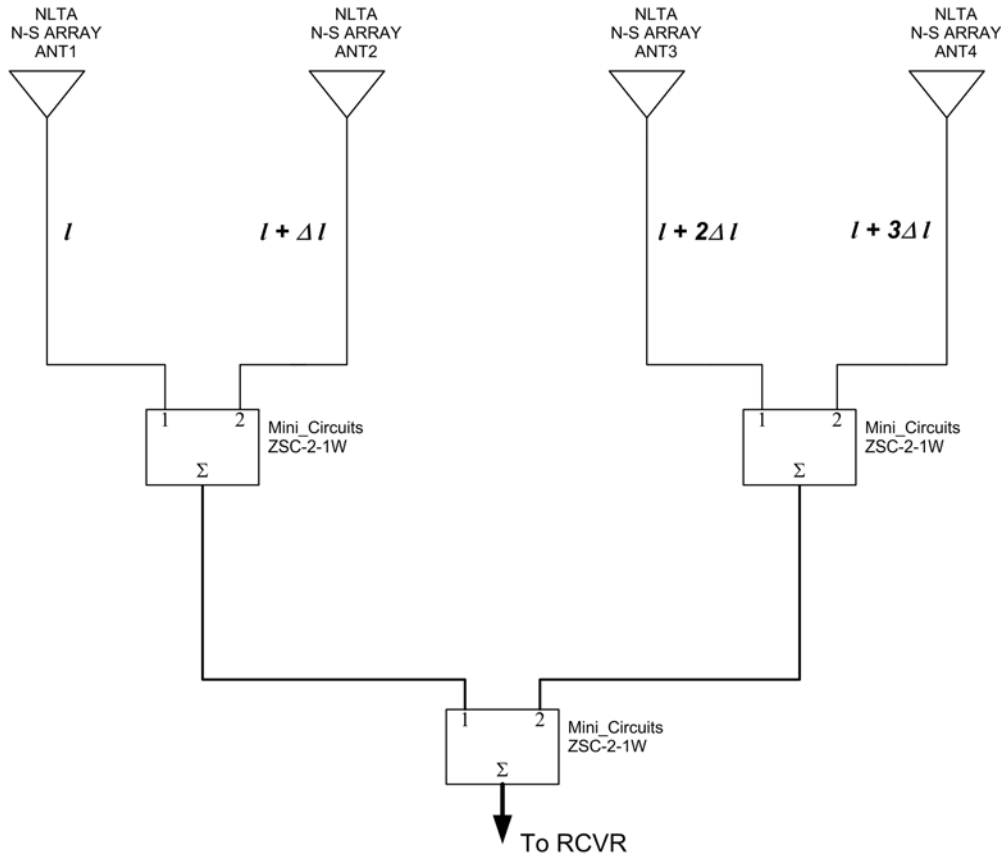


Fig. 7 — Delay lines and power combiners for north-south array beamforming

The voltages from the two four-element arrays are then summed by means of a Mini-Circuits PMT-1 $0^\circ/180^\circ$ power combiner to operate as a phase-switched (multiplying) interferometer [8]. In addition to the phase-switch output, labeled S/J in the circuit layout diagram shown in Fig. 8, the circuit board also includes two A/B switches for possible future enhancements. Figure 9 shows the schematic diagram of these circuits. An HP 141T spectrum analyzer with resolution bandwidth set to 100 kHz detects the signals. Its output is digitized (Measurements Computing, model PCI-DAS1200) and the two phases are combined in software to produce interference fringes.

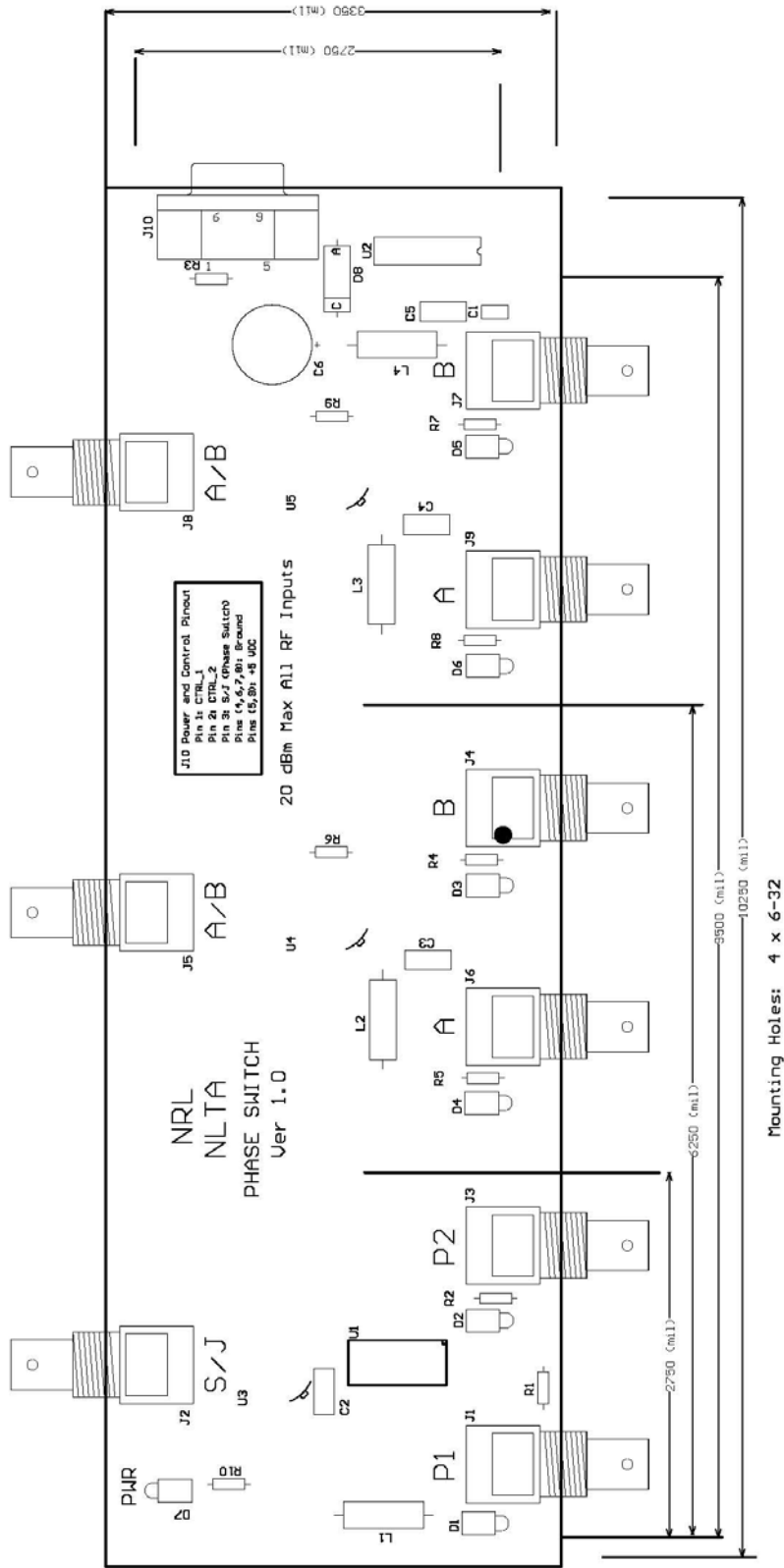


Fig. 8 — Phase switch circuit board layout

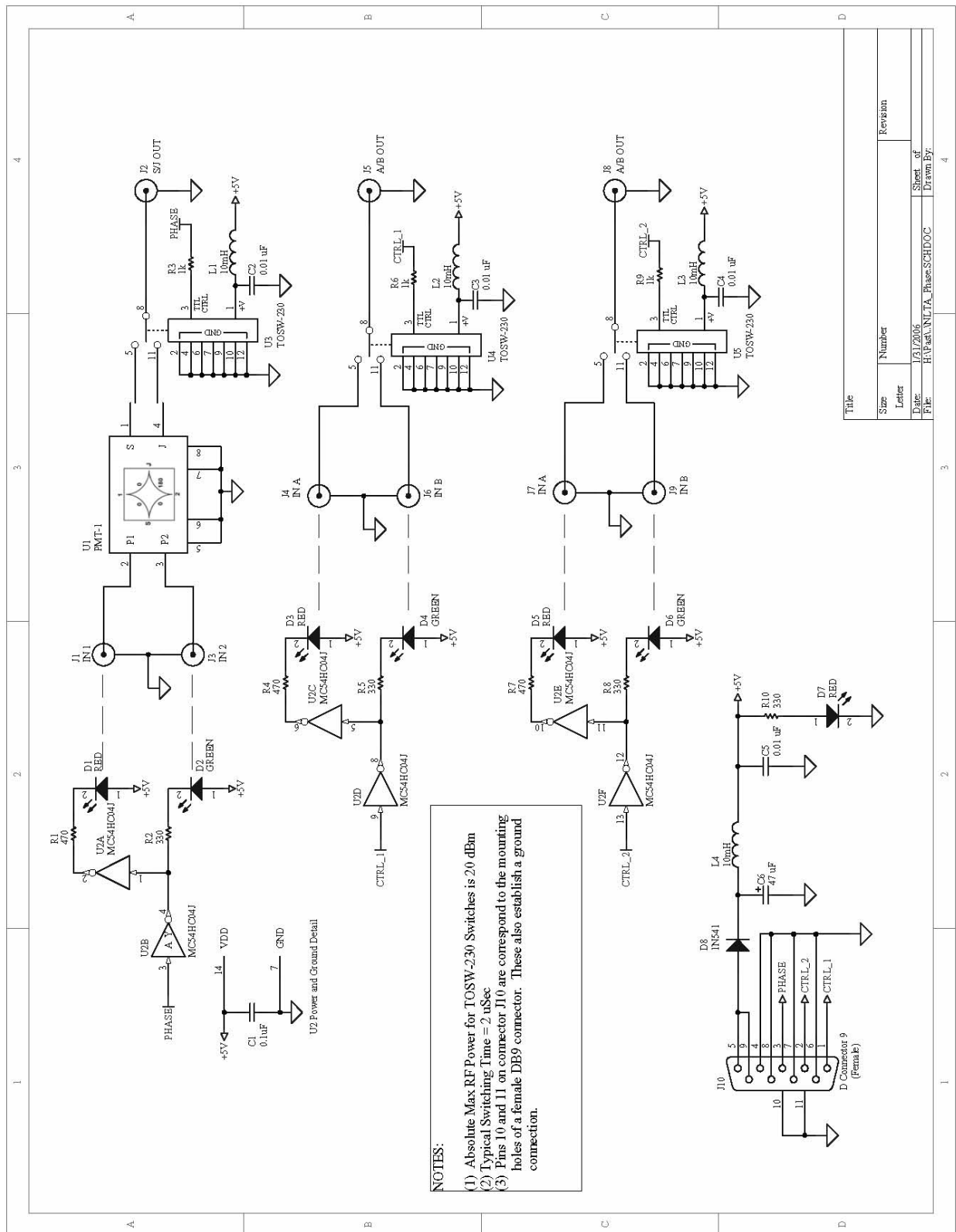


Fig. 9 — Phase switch schematic

SOFTWARE

Data collection software for the NLTA was written in C and is included in the Appendix. The software records data at five different frequencies in a serial order. The first frequency is set and the phase switch set to 0° . The software waits 20 ms for the ADC card to stabilize then reads and averages a series of data points. The phase switch is then set to 180° , the software waits another 20 ms, and another series of data is read and averaged. The difference between the data in phase and out of phase is calculated and stored in an array. The next frequency is set and the procedure repeated. After the difference has been calculated for the fifth frequency, the software loops and sets the first frequency again. This loop is repeated N times where N can be adjusted. Typically, $N = 75$ was used. When the software has looped N times over all five frequencies, the simple mean of each difference array for each frequency is calculated, though more sophisticated RFI-excising averaging may be done in the future. The time and five averages are then written to a file, the loop counter reset and the process begins again. The program runs continuously with separate data files written each day. Software was also developed to read NLTA data files and plot the fringe patterns. Figure 10 shows a typical fringe plot.

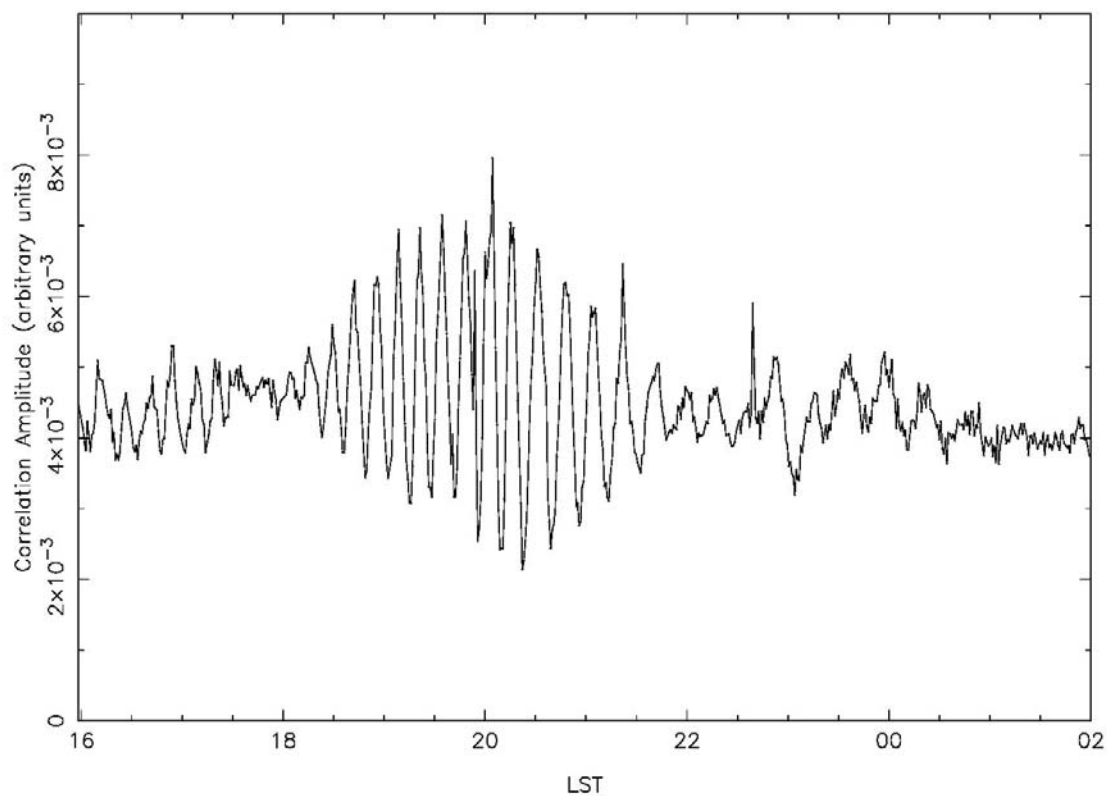


Fig. 10 — Fringes at 38 MHz observed with the NLTA. The largest fringes around 20^{h} local sidereal time (LST) are due to Cygnus A passing through the main beam. The smaller fringes between 23^{h} and 24^{h} are due to Cassiopeia A passing along the side of the main beam, where the response is -16 dB relative to the maximum.

The five observing frequencies of the NLTA were chosen to be relatively free of radio frequency interference (RFI). This was done by careful inspection of the spectrum analyzer power spectrum output

averaged over several hours. A typical scan is shown in the green curve in Fig. 11. Regions with large spikes or high variability have high RFI and were avoided. The five observing frequencies of the NLTA for most of the measurements were chosen to be 25.6, 32.0, 36.0, 38.0, and 42.0 MHz, the first and fourth of which lie in radio astronomy protected allocations.

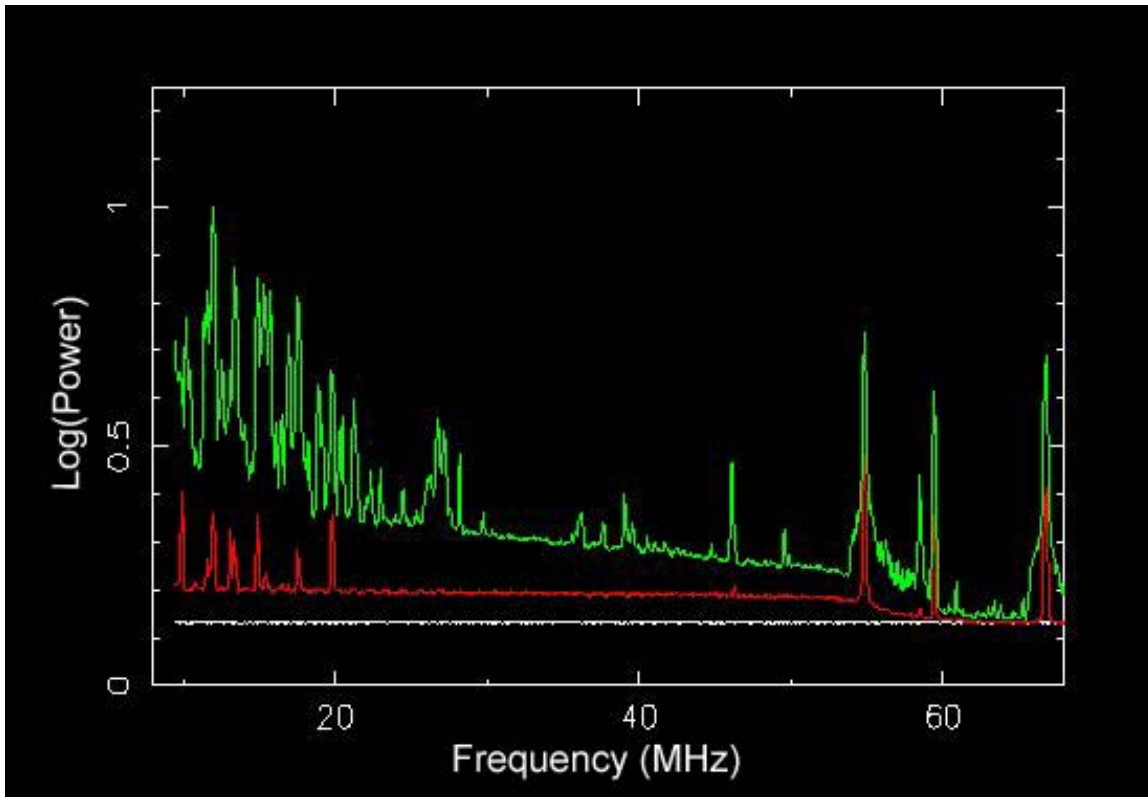


Fig. 11 — Single antenna spectrum. The curves are, from bottom to top, system noise, dummy load, and sky observations. The vertical axis is the logarithm of the signal strength in arbitrary units. The horizontal axis is the frequency in MHz.

RESULTS

Figure 11 shows a Galactic background spectrum (green curve) observed with one of the dipoles. A 50 MHz lowpass filter was used to attenuate the signals from VHF commercial broadcast stations. The lowest trace (white) is the system noise with the active balun switched off. The middle trace (red) was made with a 50- Ω load substituted for the dipole. This spectrum shows the thermal noise of the load (290 K) plus the excess noise generated by the preamp (387 K). The top trace shows the spectrum with the dipole connected and observing the sky (both Galactic and terrestrial noise). The slope of the curve is consistent with the $\nu^{-2.55}$ dependence of the Galactic brightness temperature at these frequencies [9].

In order to test the accuracy of our antenna response pattern simulations we have used the NLTA to measure the response patterns by observing, at various frequencies, several of the strongest celestial sources at different declinations as they rotated through the beam. Phasing cables, mentioned above, are used to point the beam in different directions, although digital delays are planned for the future. When signals from four of the antennas are combined in phase to form the 4×1 E-W array, the resulting pattern

is a fan beam with maximum along the meridian. For some observations, delay cables were inserted at the E-W array to direct the beam east or west of the meridian. This shifted the fringes earlier or later in the day exactly as expected. Figure 12 shows the calculated elevation response pattern through the zenith in the E-W plane. At 38 MHz, the beam width between first nulls is calculated to be 45° ; therefore, at the latitude of the NLTA site (39° N), the duration of the fringes should be 4.0 hr. The fringes in Fig. 10, observed at 38 MHz, are due to Cygnus A, which passes $< 2^\circ$ from the zenith at the latitude of the NLTA site. The duration of the fringes agrees with this prediction. Given the interferometric baseline shown in Fig. 2, there should be approximately 5 fringes per hour as Cyg A transits the meridian, also in agreement with the observations of Fig. 10.

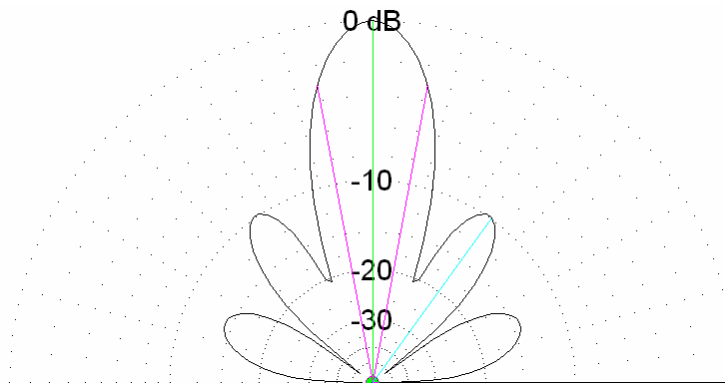


Fig. 12 — The calculated 38 MHz response pattern of the 4×1 east-west array. The first-null beam width at the zenith is 45° .

Figures 13 and 14 are dynamic spectra of two solar bursts observed with the Goddard Decametric Radio Telescope (GDRT), which uses an NLTA antenna and balun and is located adjacent to the NLTA at NASA/GSFC in suburban Washington, DC. They show that the system has sensitivity from < 12 MHz to > 60 MHz. The cutoff around 15 MHz is due to the ionosphere; we believe that these active antennas actually work down to at least 5 MHz. Although these dipoles have sensitivity up to > 110 MHz, their usefulness for astronomical observations above 50 MHz declines because the antenna response decreases at the zenith and develops strong side lobes near the horizon.

An initial version of the Green Bank Solar Radio Burst Spectrometer (GB/SRBS) at NRAO in West Virginia was constructed from an NLTA antenna combined with an NRAO active balun. Its observations of emission from B4.7 (15:29) and B5.6 (15:36) solar flares are shown in Fig. 15. Beneath the spectrograph, the solid curve is the integrated radio flux and the dashed curve is the GOES X-ray flux.

The NLTA was also used for a graduate research project by one of the authors (C. Gross) at the University of Maryland [7]. He observed the Galactic supernova remnant Cassiopeia A, which is one of the strongest discrete radio sources in the sky, and is therefore often used as an absolute flux density calibrator for radio astronomical observations. However, theory predicts, and higher frequency observations confirm, a frequency-dependent secular decrease in its radio flux density. Gross's data are consistent with such a secular decrease, although his preliminary results need to be confirmed through further measurements. His observations show a flux density decrease rate of $d_{38} \sim 0.56\%$ per year for Cas A. These measurements are valuable because the flux density is poorly constrained in the relatively low frequency range at which the NLTA operates.

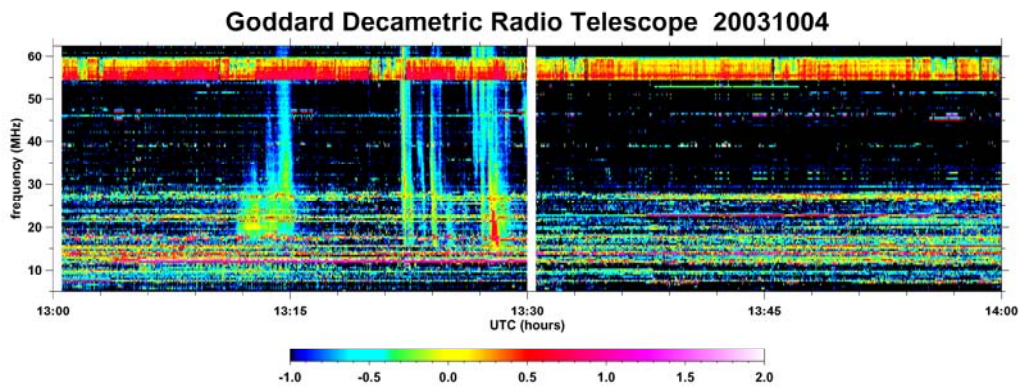


Fig. 13 — A spectrum of type III solar bursts observed with a single antenna (GDRT)

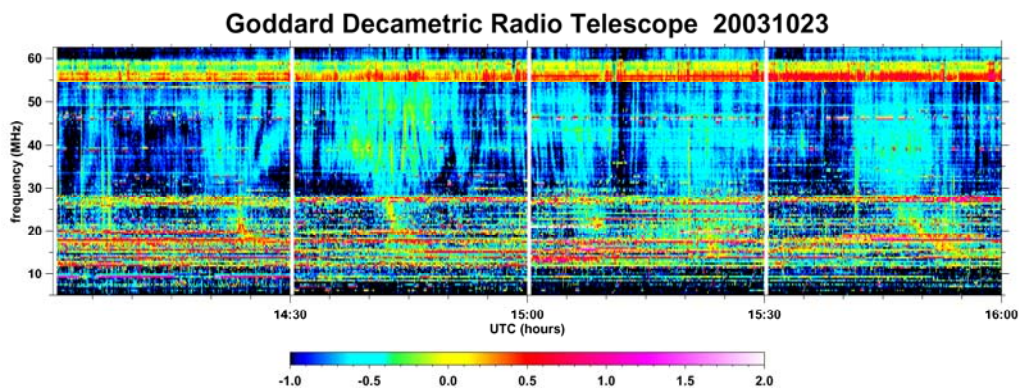


Fig. 14 — Type IV continuum (plus type III storm) with ionospheric distortions observed with a single antenna (GDRT)

CONCLUSIONS

The NLTA project has provided a valuable test bed for the technologies needed for the LWA, and allowed tests of the accuracy of numerical simulations of the antenna properties. Interferometric fringes from celestial sources agreed in duration, frequency, and relative amplitudes with theoretical predictions. Several different sized “fat” inverted-V dipoles with active baluns were tested by observing the Galactic background and the Sun. We found that they work well over the frequency range in which the dipole arms vary from about $1/8$ wavelength to one wavelength, i.e., from 15 to 115 MHz for the dipoles used in the construction of the NLTA, and even the simple NLTA technology can make useful contributions to solar radio astronomy. The low-frequency limit, apart from ionospheric absorption, appears to be set by resistive losses and low efficiencies caused by the strong coupling between the dipole and its ground image. The high frequency limit occurs where the dipole is too high above the ground screen ($\sim \lambda/2$) and its response pattern begins to develop a null at the zenith making it inappropriate for radio astronomical observations. Systems designed along these lines appear to be possible receptors for LWA in the 10 to 80 MHz range.

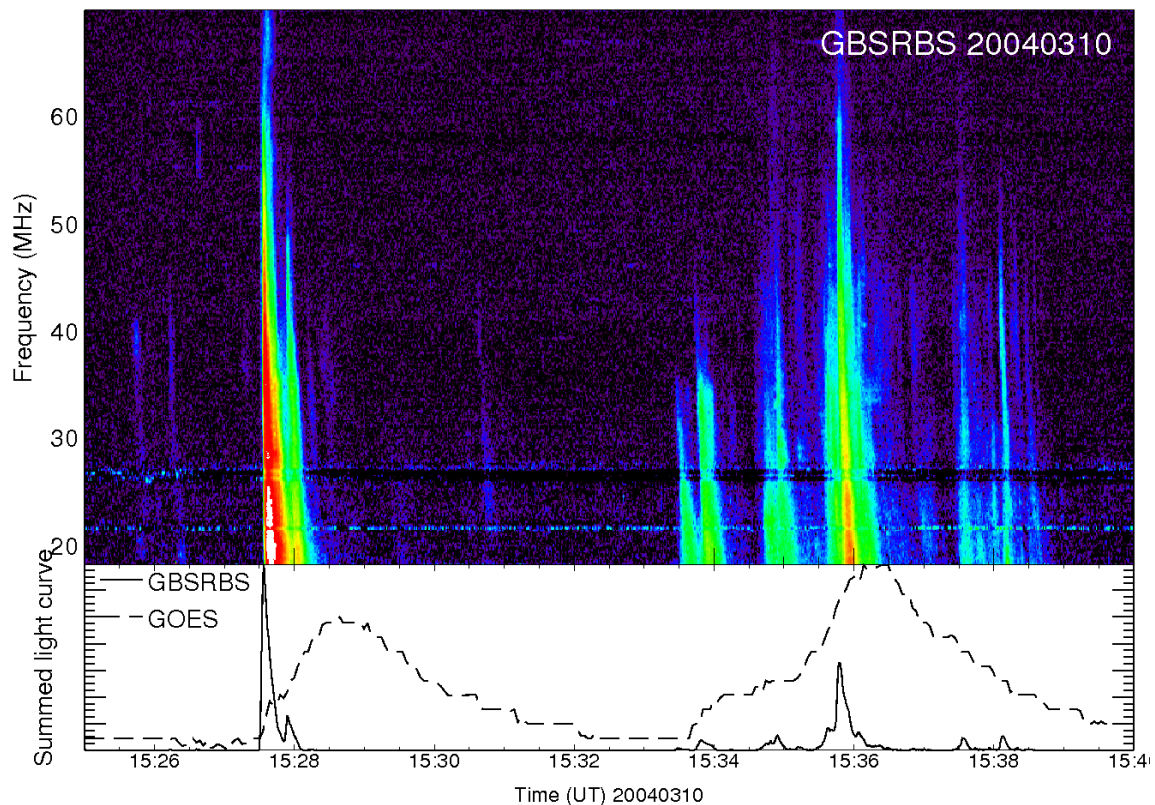


Fig. 15 — Emission from B4.7 (15:29) and B5.6 (15:36) flares observed with a single antenna (GB/SRBS) in the quieter RFI environment at NRAO in Green Bank, WV. Also shown are the integrated radio flux (solid curve) and the GOES X-ray flux (dashed line)

ACKNOWLEDGMENTS

We are grateful to R.B. MacDowall, GSFC, for permission to include the GDRT spectra, and S. White, University of Maryland, for permission to include the GB/SRBS spectrum. Research in radio astronomy at the Naval Research Laboratory is supported by funding from the Office of Naval Research.

REFERENCES

1. N.E. Kassim, T.J.W. Lasio, W.C. Erickson, P.C. Crane, R.A. Perley, and B.C. Hicks, “The Low-Frequency Array (LOFAR): Opening a New Window on the Universe,” in H.R. Butcher (ed.), *Radio Telescopes, Proc. SPIE* **4015**, 328-340 (2000).
2. N.E. Kassim, T.J.W. Lasio, P.S. Ray, P.C. Crane, B.C. Hicks, K.P. Stewart, A.S. Cohen, and W.M. Lane, “The Low-Frequency Array (LOFAR): Opening a New Window on the Universe,” *Planetary and Space Science* **52**, 1343–1349 (2004).
3. S.E. Khaikin and N.L. Kaidanovskii, “A New Radio Telescope of High Resolving Power,” in R.N. Bracewell (ed.), *Paris Symposium on Radio Astronomy* (Stanford University Press, Stanford, CA, 1959) p. 166.

4. M.F. Morales, J.N. Hewitt, J.C. Kasper, B. Lane, J. Bowman, P.S. Ray, and R.J. Cappallo, “The GRB All-sky Spectrometer Experiment (GASE),” in N.E. Kassim, M.R. Perez, W. Junor, and P.A. Henning (eds.), *From Clark Lake to the Long Wavelength Array: Bill Erickson’s Radio Science Conference Series*, Volume 345 (Astronomical Society of the Pacific, San Francisco, CA, 2005) p. 512.
5. R. Bradley, C. Parashare, S.M. White, and T.S. Bastian, “Instrument Development for the Green Bank Solar Radio Burst Spectrometer (GB/SRBS),” in N.E. Kassim, M.R. Perez, W. Junor, and P.A. Henning (eds.), *From Clark Lake to the Long Wavelength Array: Bill Erickson’s Radio Science Conference Series*, Volume 345 (Astronomical Society of the Pacific, San Francisco, CA, 2005) p. 357.
6. S.W. Ellingson, “Antennas for the Next Generation of Low Frequency Radio Telescopes,” *IEEE Trans. Antennas and Propagation* **53**, 2480 (2005).
7. C. Gross, “The Secular Decrease of Cas A at 38 MHz,” Second Year Research Project, Dept. of Astronomy, Univ. of Maryland, 2004.
8. J.D. Kraus, *Radio Astronomy*, 2nd ed. (Cygnus-Quasar, Ohio, 1986), Sec. 6-11.
9. H.V. Cane, “Spectra of the Non-thermal Radio Radiation from the Galactic Polar Regions,” *Mon. Not. R. Astron. Soc.* **189**, 465–478 (1979).

Appendix

NLTA DATA COLLECTION C CODE

```
    NLTA data collection C code
/*
 * getfringe.c
 *
 * Program to record fringes from the NLTA.
 * For each frequency take data at 0 and 180 deg phase and accumulate the
difference.
 *
 * Last modified by Emil Polisensky 8/11/03
 *
 */

/* Include files */
#include <stdio.h>
#include <unistd.h>
#include <ctype.h>
#include <math.h>
#include <time.h>
#include "calib.h"
#include "cpgplot.h"
#include "cbw.h"
#include "stat.h"
#include "nlta.h"
#include "lst.h"

void plt_txtline(int plot_id, int line, char *text, int erase);
double freq_to_volts(double freq);
double volts_to_freq(double volts);

int main(int argc, char *argv[])
{
    int WaituSec=20000; /* Number of microseconds to wait for NLTA board to
stabilize */
    int nsamp=1000; /* Take the mean of this many samples for each phase */
    int num_avg=75; /* Number of means to average for each point on fringe plot
*/
    int npts_fringe=2500; /* Number of points to display on fringe plot */
    long rate=20000; /* Sampling rate in Hz */

    char fname[256],line[256],filechar;
    FILE *outfile;
    time_t tt;
    int utdoy,utyear,uthour,utmin,utdoy_old;
    int colorset,lstmin,na,dummy1,i,index,pg_id_fringe,pg_id_raw,pg_id_text;
    WORD *rawdata0, *rawdata180;
    float *volts0,*volts180,meandiff,mean0,mean180,sum;
    float *diffarray1,*diffarray2,*diffarray3,*diffarray4,*diffarray5;
    double arave[5],lsthour;

    /* Enter the frequencies to observe at (in MHz) */
    /* double freq[]={25.6,30.9,38.0,39.0,44.0}; */
    /* Looking at tscan on Oct 1, 2003, Ken and Paul chose these freqs */

```

```

double freq[]={25.6,32.0,36.0,38.0,42.0};
/* I've changed this to observe only at 38 MHz. AC 9/12/03 */
/* double freq[]={38.0, 38.0, 38.0, 38.0, 38.0}; */

for(i=0;i<5;i++){
    printf("%f %f\n",freq[i],freq_to_volts(freq[i]));
}

rawdata0 = calloc(nsamp,sizeof(WORD));
rawdata180 = calloc(nsamp,sizeof(WORD));
volts0 = calloc(nsamp,sizeof(float));
volts180 = calloc(nsamp,sizeof(float));
diffarray1 = calloc(num_avg,sizeof(float));
diffarray2 = calloc(num_avg,sizeof(float));
diffarray3 = calloc(num_avg,sizeof(float));
diffarray4 = calloc(num_avg,sizeof(float));
diffarray5 = calloc(num_avg,sizeof(float));

/* First, setup board */
NLTA_InitMC();

/* Open plot devices */
pg_id_fringe = cpgopen("4/XSERVE");
cpgask(0);
pg_id_raw = cpgopen("2/XSERVE");
cpgask(0);
pg_id_text = cpgopen("3/XSERVE");
cpgask(0);

cpgslct(pg_id_fringe);
cpgpage();
cpgsvp(0.1f,0.95f,0.1f,0.95f);
cpgsch(2.0);
cpgswin(0.0,24.0,-.035f,.035f);
cpgtbox("XZYBC1NST",0.0,0,"BC1NST",0.0,0); /* Draw box (axes and labels) */
cpglab("Time","Power","Fringe Patterns");
cpgupdt();

/* Prepare file for writing */
tt=time(NULL);
utdoy=gmtime(&tt)->tm_yday+1;
utyear=gmtime(&tt)->tm_year+1900;
uthour=gmtime(&tt)->tm_hour+1;
utmin=gmtime(&tt)->tm_min;
utdoy_old=utdoy;
filechar='a'-1;
do{
    filechar += 1;
    sprintf(fname,"FRINGE%04d%03d%c.multi.dat",utyear,utdoy,filechar);
    if(filechar>'z'){
        fprintf(stderr,"Failed to find an unused filename!\n");
        exit(32);
    }
}while(!f_exist(fname));
printf("Opening new output file [%s]\n",fname);
outfile=fopen(fname,"a");
if(outfile==NULL){
    fprintf(stderr,"Error opening file %s\n",fname);
    exit(94);
}

```

```

/* Slow loop -- loops forever */
while (1) {
    cpghlct(pg_id_raw);
    cpghpage();
    cpghsvp(0.1f,0.95f,0.1f,0.90f);
    cpghsch(2.0);
    cpghswin(0.0, (float)num_avg, -0.2f, 0.8f);
    cpghbox("BC1NST",0.0,0,"BCNST",0.0,0);
    cpghlab("Time", "Power", "Raw Data");

    /* Update text plot */
    lstmin = 60 * modf(Unix_to_LST(tt)/3600, &lsthour);
    plt_txtline(pg_id_text, 1, "FRINGE 1.0", 1);
    sprintf(line, "The LST is %2.0f:%02d ", lsthour, lstmin);
    plt_txtline(pg_id_text, 2, line, 0);
    sprintf(line, "Light blue = %.1f MHz", freq[0]);
    plt_txtline(pg_id_text, 3, line, 0);
    sprintf(line, "Purple = %.1f MHz", freq[1]);
    plt_txtline(pg_id_text, 4, line, 0);
    sprintf(line, "Yellow = %.1f MHz", freq[2]);
    plt_txtline(pg_id_text, 5, line, 0);
    sprintf(line, "Orange = %.1f MHz", freq[3]);
    plt_txtline(pg_id_text, 6, line, 0);
    sprintf(line, "Green = %.1f MHz", freq[4]);
    plt_txtline(pg_id_text, 7, line, 0);
    cpghupdt();

    /* Fast loop */
    for (na=0; na<num_avg; na++) {

        for (index=0; index<5; index++){ //loop over frequencies
            /* Set frequency */
            NLTA_SetScanVoltage(freq_to_volts(freq[index]));

            /* Set phase 0deg */
            NLTA_SetPhase0();
            usleep(WaituSec);

            /* Read and average a block of data */
            NLTA_ReadDetVoltageN(nsamp,rate,rawdata0,volts0);
            mean0 = RobustMean(nsamp,volts0);

            /* Set phase 180deg */
            NLTA_SetPhase180();
            usleep(WaituSec);

            /* Read and average a block of data */
            NLTA_ReadDetVoltageN(nsamp,rate,rawdata180,volts180);
            mean180 = RobustMean(nsamp,volts180);

            /* Now, calculate difference between 0 and 180 deg phases */
            meandiff = mean0 - mean180;

            /* Store difference in an array */
            switch(index){
            case 0:
                diffarray1[na] = meandiff;
                break;
            case 1:

```

```

        diffarray2[na] = meandiff;
        break;
    case 2:
        diffarray3[na] = meandiff;
        break;
    case 3:
        diffarray4[na] = meandiff;
        break;
    case 4:
        diffarray5[na] = meandiff;
        break;
    default:
        printf("error in inner loop! index went too high!\n");
        fflush(stdout);
        break;
}

/* Plot points on raw plot for each frequency */
cpgslct(pg_id_raw);
cpgsci(2); /* Red */
cpgpt1((float)na, mean0,1);
cpgsci(3); /* Green */
cpgpt1((float)na, 1.0*mean180,1);
cpgsci(4); /* Blue */
cpgpt1((float)na, meandiff,1);
cpgsci(1);

    } /* end of "index" for loop */

} /* end of fast loop */
cpgupdt();

/* Calculate the mean of each diffarray and add to plot */
/* Calculates simple means, some kind of RFI filtering should eventually
be done */
for (index=0; index<5; index++){
    sum = 0.0;
    for (dummy1=0; dummy1<num_avg; dummy1++){
    switch(index){
    case 0:
        sum = sum + diffarray1[dummy1];
        break;
    case 1:
        sum = sum + diffarray2[dummy1];
        break;
    case 2:
        sum = sum + diffarray3[dummy1];
        break;
    case 3:
        sum = sum + diffarray4[dummy1];
        break;
    case 4:
        sum = sum + diffarray5[dummy1];
        break;
    default:
        printf("error in averaging loop!\n");
        fflush(stdout);
        break;
    }
}
}

```

```

    arave[index]=sum/num_avg;
}

tt=time(NULL);
utdoy=gmtime(&tt)->tm_yday+1;
uthour=gmtime(&tt)->tm_hour+1;
utmin=gmtime(&tt)->tm_min;
if(utdoy != utdoy_old){
    /* open a new file */
    fclose(outfile);
    filechar='a'-1;
    do{
filechar+=1;
utyear=gmtime(&tt)->tm_year+1900;
sprintf(fname, "FRINGE%04d%03d%c.multi.dat", utyear, utdoy, filechar);
if(filechar>'z'){
    fprintf(stderr, "Failed to find an unused filename!\n");
    return(53);
}
    }while(f_exist(fname));
    printf("Opening new output file [%s]\n", fname);
    outfile=fopen(fname, "a");
    if(outfile==NULL){
fprintf(stderr, "Error opening file %s\n", fname);
exit(94);
    }
    printf("Writing file at (%ld) UTC %s", tt, asctime(gmtime(&tt)));
    fflush(outfile);
    utdoy_old=utdoy;
}

/* Add points to fringe plot, a different color for each frequency */
cpgslct(pg_id_fringe);
colorset=5;
for(index=0; index<5; index++){
    cpgsci(colorset);
    cpgpt1(Unix_to_LST(tt)/3600.0, arave[index], 1);
    colorset++;
}
cpgupdt();

/* write time, and arave[], to file */

fprintf(outfile, "%ld\t%12.5f\t%12.5f\t%12.5f\t%12.5f\t%12.5f\n", tt, arave[0], arave[1], arave[2], arave[3], arave[4]);
    fflush(outfile);

} /* end of slow loop */
cpgend();
exit(0);

} //end of main

/* Put a line of text into the info window*/
void plt_txtline(int plot_id, int line, char *text, int erase)
{
    cpgslct(plot_id);

    if (erase)

```

```
    cpqpage();

    cpqsch(2.5);
    cpqsvp(0.05f,0.98f,0.12f,0.98f);
    cpqswin(0.0,1.0,0.0,1.0);
    cpqmtxt("T",-1.0f*(float)line,0.05f,0.0f,text);

    return;
}

/* Convert a frequency to a voltage using the current calibration */
double freq_to_volts(double freq)
{
    double volts;

    volts=(freq - CALIB_INTERCEPT)/CALIB_SLOPE;
    return volts;
}

/* Convert a voltage to a frequency using the current calibration */
double volts_to_freq(double volts)
{
    double freq;

    freq=CALIB_SLOPE*volts + CALIB_INTERCEPT;
    return freq;
}
```